Toxicology Letters 413 (2025) 111743

Contents lists available at ScienceDirect

Toxicology Letters

journal homepage: www.journals.elsevier.com/toxicology-letters

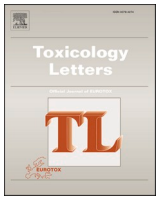

Differentiating the *in vitro* toxicity of solid-surface composite dust: A comparison of material components and abrasive particles

W. Kyle Mandler [a,*], Walter McKinney [a], Chaolong Qi [b], Alycia Knepp [a], Eun Gyung Lee [c], Seungkoo Kang [b], Sarah Keeley [a,b,c], Yong Qian [a]

[a] *Health Effects Laboratory Division, National Institute for Occupational Safety and Health, Morgantown, WV, United States*
[b] *Division of Field Studies and Engineering, National Institute for Occupational Safety and Health, Cincinnati, OH, United States*
[c] *Respiratory Health Division, National Institute for Occupational Safety and Health, Morgantown, WV, United States*

ARTICLE INFO

Keywords:
Solid-surface composite
Aluminum trihydrate
Particulates
in vitro toxicity
Aluminum oxide

ABSTRACT

Background: Workers fabricating solid-surface composite (SSC) materials like Corian® are exposed to airborne particulate matter (PM) containing aluminum trihydrate (ATH) and potentially abrasive particles from sanding tools, leading to concerns about respiratory health effects like pulmonary fibrosis. However, the relative toxicological contributions of the SSC material versus the sandpaper abrasives remain unclear.
Objective: This study aimed to compare the *in vitro* cellular responses induced by respirable dust generated from sanding SSC with different commercial sandpapers (aluminum oxide [Al2O3], ceramic, silicon carbide [SiC]) to the responses elicited by ATH and corresponding abrasive analogue particles.
Methods: Respirable dust (PM with an aerodynamic diameter less than 5 μm) was generated from sanding Corian® using the three sandpaper types via a fluidized bed generator coupled with a cyclone separator. Human monocytic THP-1 cells, differentiated into macrophage-like cells, were exposed for 48 h to suspensions of these SSC dusts, ATH, or Al2O3, ceramic, and SiC abrasive analogue particles (10 μg/well). Cytotoxicity (LDH release), apoptosis (Caspase 3/7 activity), necrosis (propidium iodide uptake), cell cycle distribution, and nuclear morphology (including mono-, bi-, multi-, and micronucleation) and the Nuclear Division Index were assessed.
Results: Exposure to SSC dusts generated with any sandpaper type, as well as ATH, resulted in significant increases in apoptosis compared to controls. However, these exposures did not cause significant LDH release or alterations in cell cycle progression or mitotic indices. Conversely, the Al2O3, ceramic, and SiC abrasive analogue particles induced significant disruptions in cell cycle (S phase population reduction) and mitosis (increased multinucleation, micronucleation, and NDI), alongside apoptosis (Al2O3, SiC) or necrosis (ceramic, SiC), but also caused minimal LDH release.
Conclusion: Under these *in vitro* conditions, the apoptotic response to respirable SSC sanding dust appears primarily driven by components inherent to the SSC material itself, consistent with the effects of ATH. This response profile was distinct from the cell cycle arrest and mitotic disruption prominently caused by the abrasive analogue particles. These findings suggest the intrinsic properties of SSC material components are key drivers of initial macrophage responses *in vitro*, differing significantly from the effects of the abrasive materials alone.

1. Introduction

Solid-surface composite (SSC) is a material that has been used increasingly in countertops, sink basins, furniture, building cladding, and a variety of other applications (DuPont, 2018). Aluminum trihydrate (up to 70 % by weight) and acrylate polymers are two major components of some SSCs. Working with these materials during manufacturing of SSC products and fabricating them using sawing and sanding into final products can release a large amount of PM and volatile organic compounds (VOCs). Exposure to aluminum PM has been associated with pulmonary fibrosis (Hubbard et al., 2000, Jederlinic et al., 1990, Taskar and Coultas, 2006). Raghu et al. (2014) reported a fatal case of pulmonary fibrosis in a worker who ground, machine-drilled and sanded SSC for 16 years. This case was associated with the inhalation of

* Corresponding author.
E-mail address: oex1@cdc.gov (W.K. Mandler).

https://doi.org/10.1016/j.toxlet.2025.111743
Received 18 June 2025; Received in revised form 25 September 2025; Accepted 10 October 2025
Available online 13 October 2025
0378-4274/Published by Elsevier B.V.

aluminum trihydrate. Chew et al. (2016) also reported a case of alveolar proteinosis associated with the inhalation of aluminum PM.

The toxicological effects of the airborne contaminants from working with SSC have not been fully investigated. Our previous in vivo studies showed that oropharyngeal aspiration of 500 and 1000 μg of PM from sawing SSC induced pulmonary inflammation and collagen deposition in mice. Moreover, we found that alveolar particle deposition and granulomatous mass formation occurred in all exposed mice at 14 days post-exposure, and the SSC particles were poorly cleared from the mice lungs, with 81 % remaining after 14 days post exposure (Mandler et al., 2019). Our whole-body inhalation exposure studies showed that exposure to SSC cut dust at 20 mg/m^3 for 4 days, 4 h/day induces mild transient inflammation up to 56 days post-exposure (Mandler et al., 2025). To determine the toxicity of the PM of different size fractions from sawing SSC, human alveolar macrophages (THP-1) were exposed *in vitro* to five size fractions (0.07, 0.66, 1.58, 5.0, and 13.42 μm diameter) of the PM. Results showed a size-dependent cytotoxic effect in the cells exposed to the PM from sawing SSC, with the smallest size fraction showing the greatest toxicity (Mandler et al., 2020).

The reported pulmonary fibrosis case (Raghu et al., 2014) was associated with aluminum trihydrate PM deposited in the lung following years of working with SSC. However, it was not clear whether the pulmonary fibrosis was caused mainly by the aluminum trihydrate from the SSC material, or from the aluminum oxide in the sandpaper, as both substances were detected in the patient's lungs and are known to potentially contribute to pulmonary fibrosis (McKeever et al., 2014). The contributions of other chemicals from the composite materials and machining tools to the potential toxicological health effects also remain unknown. Therefore, it is especially important to identify the sources of toxicity and their specific contributions to the pulmonary injuries among the components emitted from working with SSC. Kang *et al.* (et al.2021) recently compared the PM from sanding SSC with three types of sanding paper (ceramic, aluminum oxide and silicon carbide), and reported that the use of aluminum oxide sandpaper does not result in a higher aluminum content in the PM, suggesting that the aluminum content of the PM originates from the SSC material itself. This ambiguity raises a fundamental question for occupational health: is the primary hazard driven by the intrinsic properties of the SSC material itself, or by the abrasive particles released from the sanding tools? The relative toxicological contributions of the material versus the abrasives have not been investigated. We aimed to achieve this by directly comparing the *in vitro* cellular responses to respirable dusts generated from sanding SSC with three different abrasives against the responses elicited by the primary SSC component (ATH) and the pure abrasive analogue particles alone. This approach allows for the systematic differentiation of the toxicological contributions of each potential source.

Alveolar macrophages (AM) have a critical role in the recognition, processing, and elimination of inhaled particulate matter. AM are able to phagocytize unopsonized nonbiologic particles using specialized scavenger receptors (Arredouani et al., 2006) and activate innate immune responses via toll-like receptors (Becker et al., 2002). AM exposure to PM induces the release of proinflammatory mediators to the lung, including tumor necrosis factor alpha (Mukae et al., 2000), interleukin-1β, and interleukin-6 (Hogg and Van Eeden, 2009). Some types of PM, such as silica (Hamilton et al., 2008) and diesel exhaust (Hiura et al., 1999) may also induce apoptosis in AM. Keeping in mind the important role AM play in the pulmonary response to PM exposure, the human monocyte-derived THP-1 cell line was chosen as the *in vitro* AM model for this study.

2. Materials and methods

2.1. SSC particle generation and collection

As previously described by Kang et al. (2021), we mounted a belt sander in a testing chamber and operated it automatically. PM samples were collected from sanding a Corian board with three types of sandpapers of the same grit size of 120 from the same manufacturer (Red Label Abrasives, Belding, MI): ceramic, aluminum oxide and silicon carbide. The mass-based PM size distribution from the three types of sandpapers was found to be near identical and consistently bimodal, with the first mode at about 2.5 μm and the second at about 7.5 μm. Size-classified elemental analysis revealed that the aluminum content did not vary much with either particle size or sandpaper type, and it generally agreed with the aluminum content in SSC.

2.2. Respirable dust separation system

The respirable portion of the three types of bulk SSC dust generated by sanding was separated by using a custom laboratory system. A diagram of this system is shown in Fig. 1. The design of the aerosol separation system was based on a modified version of a previously developed system (McKinney et al., 2013). In brief, the generation system, combined air flow controllers, aerosol particle monitors, data acquisition devices, and custom software with automatic feedback control to achieve constant and repeatable aerosol concentration and particle size distribution. The generator suspends particles in an air stream (15 L/min) via gentle vibrations (50–60 Hz) of bulk dust placed on a flexible latex diaphragm. Particles with aerodynamic diameters larger than 20 μm generally do not escape this generator. After leaving the generator the air and particle mixture was introduced into a venturi stage that dilutes and disperses the particles with an additional 17 L/min of clean air. The output of the venturi stage was 32 L/min total. The aerosol mass concentration leaving the venturi stage was continuously monitored with a Data RAM (DR-40000, Thermo Electron Co.). This instrument was utilized for real-time feedback to ensure a stable aerosol output throughout the collection period, while definitive particle size and mass distribution were determined separately using a micro-orifice uniform deposit impactor (MOUDI, Model 110 R, MSP Corp.). A third mass flow controller was connected to house vacuum and set to pull 30 L/min of flow through, first, a cyclone with a cut point of 5 μm (URG-2000–30EP, URG Corp.), then second, a custom filter holder. The filter used for collection of the respirable portion was a 142 mm diameter PTFE membrane filter with a pore size of 0.2 μm. (GTTP14250, MilliporeSigma).

The respirable dust collection system would operate continually for six hours for each collection run. The cyclone was cleaned after each run. A stainless-steel scoopula with a very gentle downward pressure was used to scrape the dust off the filter and placed into an airtight glass jar. This process was repeated until enough dust was collected.

To verify the size of the particles being collected, several particle mass size measurements were made with samples from the air exiting the cyclone. This was achieved using MOUDI. Greased foils were used for the MOUDI stages. MOUDI readings were taken with a freshly cleaned cyclone and after 6 h of continuous use. Fig. 1 shows the mass distribution for the SSC particles leaving the cyclone. There was not a significant difference between the readings. The mass median aerodynamic diameter (MMAD) of the dust being delivered to the filter was 2.78 μm with a geometric standard deviation of 2.27 with a clean cyclone, and after 6 h of use the MMAD was 2.98 μm with a geometric standard deviation of 2.23. In both cases the total mass of particles less than the 5.6 μm MOUDI stage was 93.7 %.

2.3. Cell culture

THP-1 cells (a human acute monocytic leukemia cell line) were purchased, cultured, and transformed according to the methods described previously (Mandler et al., 2020). The cells were exposed to 100 μl of 100 μg/ml respirable fraction of SSC (10 μg/well) for 48 h.

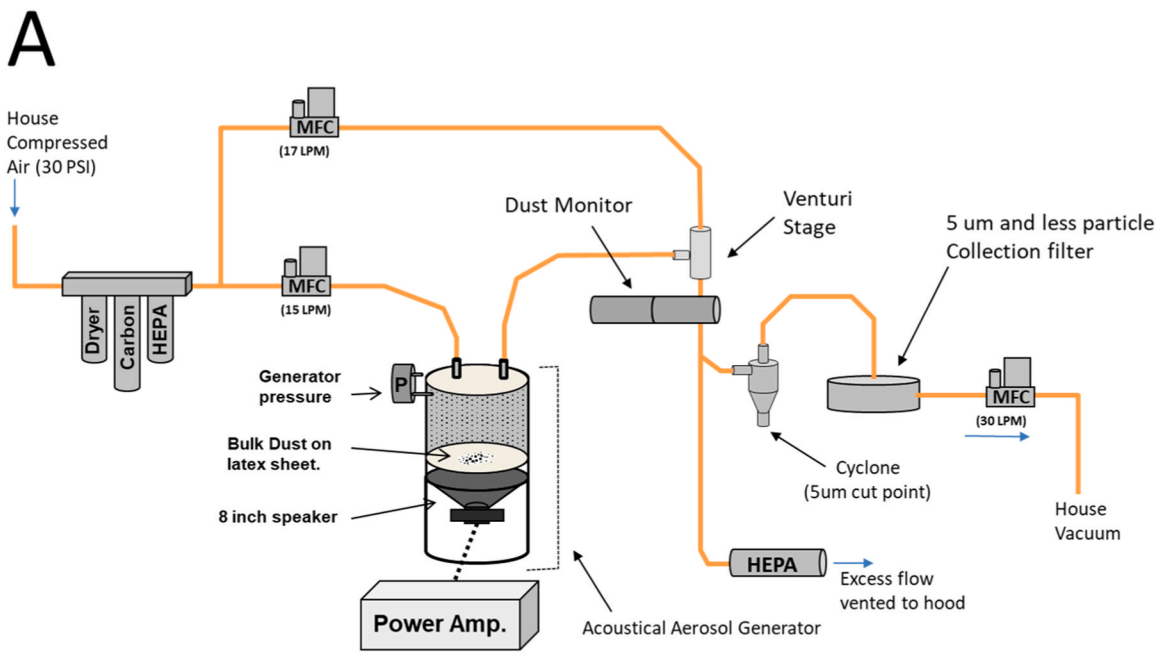

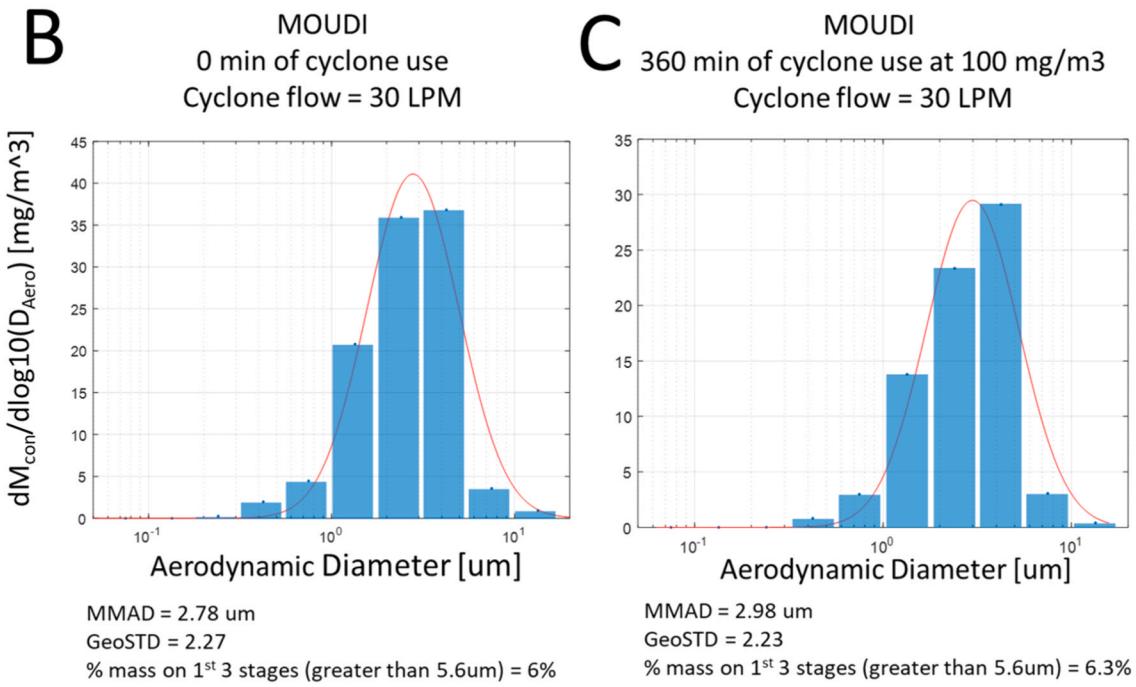

Fig. 1. Aerosol generation system and particle size characterization. (A) Schematic diagram of the custom laboratory system used to generate and isolate the respirable (< 5 μm aerodynamic diameter) fraction of Corian® dust. Key components include an acoustical aerosol generator suspending bulk dust (15 L/min flow), a venturi stage for dilution and dispersion (additional 17 L/min flow), a cyclone with a 5 μm cut point (30 L/min flow), and a final particle collection filter. (B) Particle mass size distribution measured by MOUDI after the cyclone at the start of a collection run (0 min, clean cyclone), showing MMAD = 2.78 μm and GSD = 2.27. (C) Particle mass size distribution measured by MOUDI after 6 h (360 min) of continuous generator operation, showing MMAD = 2.98 μm and GSD = 2.23. The consistent distributions demonstrate stable aerosol output over the 6-hour collection period, with > 93 % of the particle mass below 5.6 μm.

2.4. Abrasive reference particles

During the process of sanding, it is possible that the abrasives embedded in the sandpapers may dislodge and be mixed with the collected dust. In order to determine if any observed cytotoxicity may be the result of these particles, rather than the SSC particles, we obtained commercially available Aluminum oxide (Al_2O_3), aluminosilicate (AlSi, ceramic), and silicon carbide (SiC) reference particles from American Elements (Los Angeles, CA). Manufacturer information for each particle can be found in Table 1. The cells were cultured as described above and exposed to 100 μl of 100 μg/ml of each control particle (10 μg/well) for 48 h, n = 6 for each test article.

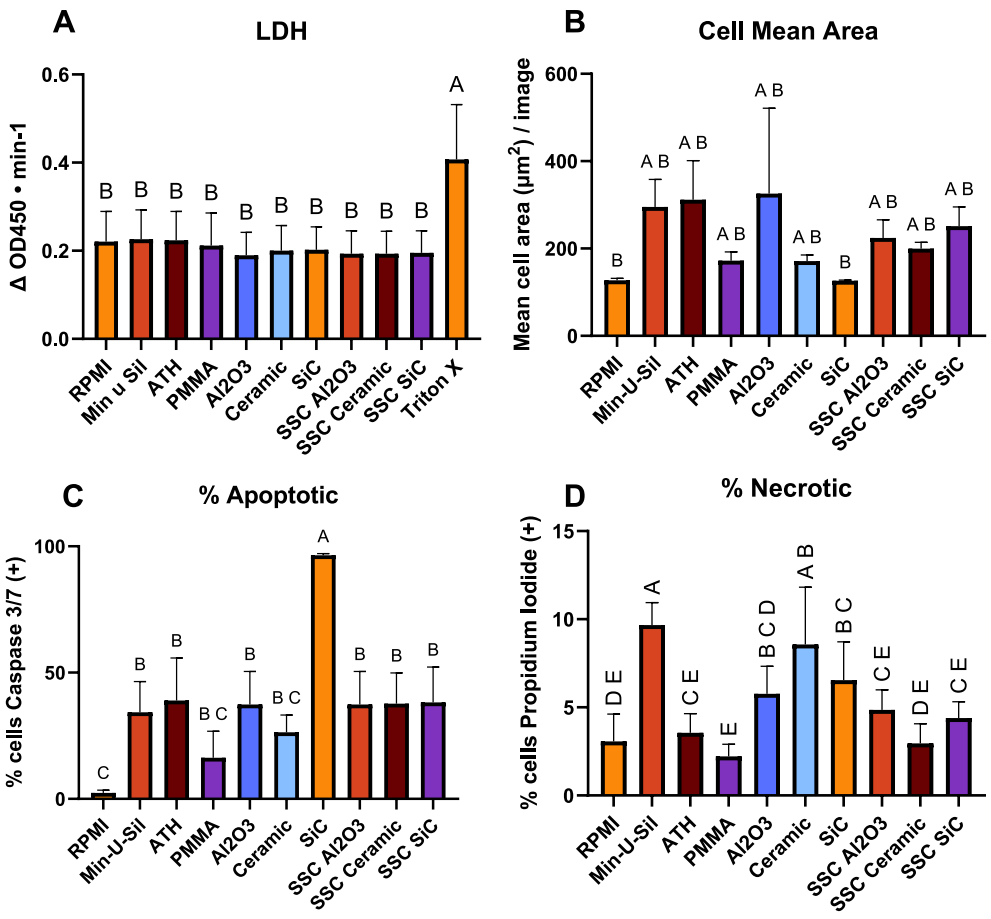

Fig. 2. Assessment of cytotoxicity, cell area, apoptosis, and necrosis following SSC sanding material exposure. Bar charts show (A) Lactate dehydrogenase (LDH) release, mean cell area per image, (C) Percentage of apoptotic cells (% Caspase 3/7 positive), and (D) Percentage of necrotic cells (% propidium iodide positive) after exposure to various materials (RPMI, Min-U-Sil, ATH, PMMA, Al2O3, Ceramic, SiC, SSC Al2O3, SSC Ceramic, SSC SiC). RPMI served as a negative control, and Triton X (Panel A) as a positive control for cytotoxicity. Data are presented as mean ± standard deviation (SD), n = 6. Letters above bars indicate statistically significant differences between groups ($p < 0.05$).

2.5. LDH activity assay

Cell culture supernatant LDH activity, a measure of cell membrane integrity and particle cytotoxicity, was measured using a lactate dehydrogenase (liquid) reagent set (Pointe Scientific, Canton, MI) according to manufacturer instructions. Briefly, 20 µl of culture supernatant was added to 200 µl reagent in a pre-warmed 96-well plate. After 5 min of incubation at 37 °C, absorbance at 450 nm was read. Following a subsequent 60-second incubation, the plate was read again at the same wavelength.

2.6. High content imaging

Following the 48-hour particle exposure, cells were incubated for 30 min with a staining solution containing Hoechst 33342 (for nuclear staining), CellEvent™ Caspase-3/7 Green Detection Reagent (for apoptosis detection, Thermo Fisher Scientific), and propidium iodide (Invitrogen, for necrosis/membrane integrity). After staining, images of the cells were acquired using an ImageXpress Confocal HT.ai High-Content Imaging System (Molecular Devices, San Jose, CA). Automated image analysis was performed using the integrated MetaXpress High-Content Image Acquisition and Analysis Software. Specific software modules were employed for quantitative analysis according to manufacturer instructions: the Multi-wavelength Cell Scoring module was used to determine the percentage of apoptotic (Caspase 3/7 positive) and necrotic (propidium iodide positive) cells; the Cell Cycle module was used to classify cells into G0/G1, S, G2, and M phases based on nuclear staining intensity; and the Micronuclei module was used to quantify micronucleated cells, assess nuclear morphology (mono-, bi-, multi-nucleated cells), and calculate the Nuclear Division Index (NDI).

2.7. Statistical analysis

A Normal Quantile-Quantile plot was used to evaluate the distribution of data sets, which were determined to be normally distributed. A simple 2-way analysis of variance (ANOVA) was performed to compare the main effects for each variable. When significant main effects were observed, a Tukey post hoc test was used to determine where significant differences existed between the groups. Technical replicates were conducted in duplicate, n = 6 for each experiment. In all cases, $p < 0.05$ was used to establish statistical significance. All data are reported as mean ± SD.

2.8. Endotoxin detection

Endotoxin was measured using Pierce™ LAL Chromogenic Endotoxin Quantitation Kits (Thermo Scientific; Waltham, MA). A standard curve was generated using the provided endotoxin as a standard, according to the manufacturer's instructions. The level of endotoxin for all samples was below the detection limit of 0.05 EU/ml.

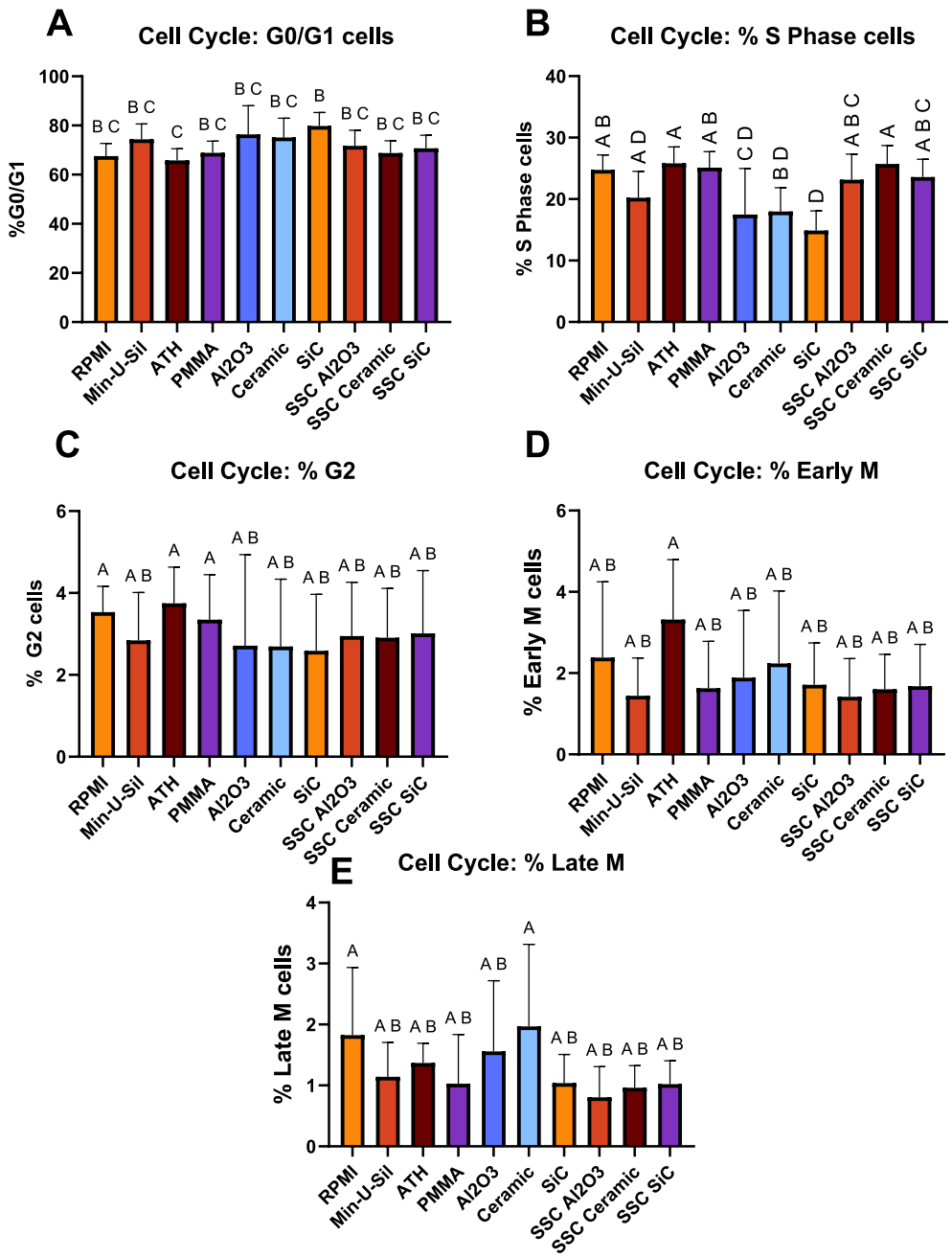

Fig. 3. Effects of SSC sanding materials on cell cycle distribution. Bar charts represent the mean percentage of cells in (A) G0/G1 phase, (B) S phase, (C) G2 phase, (D) Early M phase, and (E) Late M phase following treatment with RPMI (control), Min-U-Sil, ATH, PMMA, Al2O3, Ceramic, SiC, SSC Al2O3, SSC Ceramic, and SSC SiC. Data are presented as mean ± standard deviation (SD) for n = 6 replicates per group. Letters above bars denote statistically significant differences between groups ($p < 0.05$).

3. Results

3.1. Cytotoxicity, cell area, apoptosis, and necrosis (Fig. 2)

Cytotoxicity, assessed by lactate dehydrogenase (LDH) release, was not significantly increased by any of the tested SSC dusts or control particles compared to the RPMI negative control; only the Triton X positive control showed a significant increase. Furthermore, no significant changes in mean cell area were observed across any treatment groups. However, markers of programmed cell death were affected. Apoptosis, measured by Caspase 3/7 activation, was significantly increased by exposure to Min-U-Sil, ATH, Al2O3 particles, SiC particles, and all three types of SSC dusts (SSC Al2O3, SSC Ceramic, SSC SiC) compared to controls. Exposure to neat ceramic particles and PMMA did not significantly increase apoptosis. Notably, the neat SiC abrasive particles induced a significantly greater increase in apoptosis than the other treatments. Necrosis, indicated by propidium iodide uptake, was significantly increased only by exposure to Min-U-Sil, neat ceramic particles, and SiC particles.

3.2. Cell cycle distribution (Fig. 3)

Analysis of cell cycle progression revealed specific alterations induced primarily by the neat abrasive materials. No significant changes were detected in the percentage of cells in the G0/G1 phase across any treatment groups. However, the percentage of cells in the S phase was

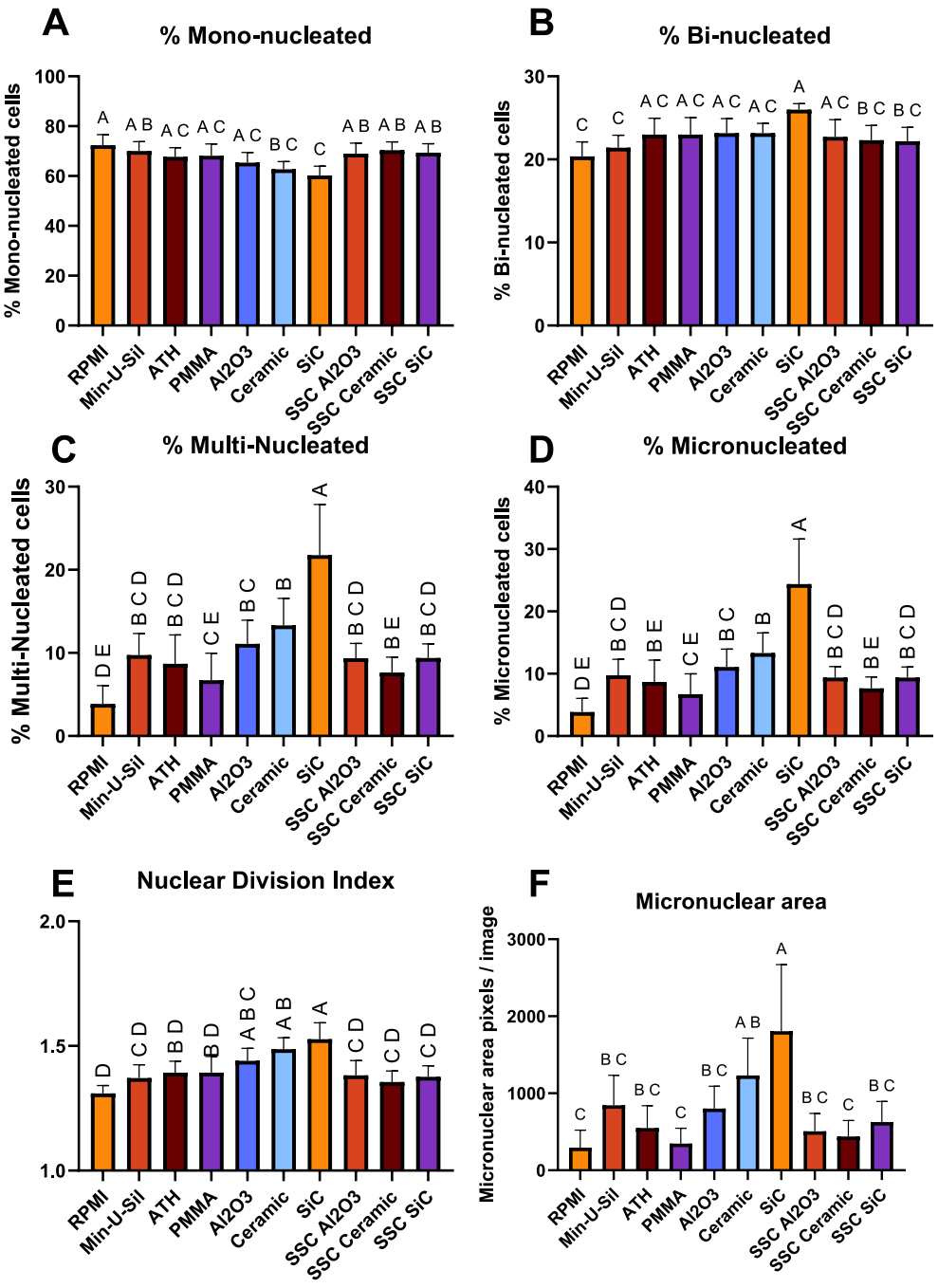

Fig. 4. Assessment of nuclear morphology and division metrics after exposure to SSC sanding materials. Bar charts represent the mean percentage of (A) mono-nucleated, (B) bi-nucleated, (C) multi-nucleated, and (D) micronucleated cells, (E) the Nuclear Division Index (NDI), and (F) the micronuclear area (pixels/image) following treatment with RPMI (control), Min-U-Sil, ATH, PMMA, Al2O3, Ceramic, SiC, SSC Al2O3, SSC Ceramic, and SSC SiC. Error bars indicate standard deviation. Letters above bars denote statistically significant differences between groups ($p < 0.05$). n = 6 for all groups.

Table 1
Abrasive and SSC matrix reference particles.

Name	Product Code	Reported Size
Silicon Carbide Nanopowder	SI-C-02M-NP.800NS	800 nm
Aluminum Oxide Powder	AL-OX-03M-P.1T2UM	1–2 μm
Aluminum Silicate Nanopowder	AL-SIAT−01-NP	0.5–1.2 μm
Alumina Trihydrate	AL-OH-04M-P	2–10 μm
PMMA Microspheres	NPM−1000–24	1.0 μm (± 3 %)

significantly reduced following exposure to the neat Al2O3, ceramic, and SiC abrasive particles. Importantly, none of the dusts generated from sanding SSC (SSC Al2O3, SSC Ceramic, SSC SiC) significantly altered the percentage of cells in S phase compared to controls. No other significant changes in the percentages of cells in the G2, Early M, or Late M phases were detected for any treatment group.

3.3. *Nuclear morphology and division (Fig. 4)*

Exposure to abrasive analogues, but not the SSC dusts, resulted in significant alterations in nuclear morphology and cell division metrics. The percentage of mononucleated cells was significantly decreased

following exposure to neat ceramic and SiC particles. Correspondingly, the percentage of binucleated cells was increased significantly only by SiC particle exposure. An increase in multinucleated cells was observed following exposure to neat Al2O3, ceramic, and SiC particles, with SiC particles inducing this effect to a significantly greater extent; none of the SSC dusts significantly increased multinucleation. A similar pattern was observed for micronucleated cells, with significant increases caused by neat Al2O3, ceramic, and SiC particles, but not by any of the SSC dusts. Consistent with these morphological changes, the Nuclear Division Index (NDI) was significantly increased by neat Al2O3, ceramic, and SiC particles, indicating disrupted cytokinesis, while SSC dusts did not significantly affect the NDI. Finally, the micronuclear area was significantly increased only by exposure to neat ceramic and SiC particles.

4. Discussion

This study investigated the source of cellular toxicity from airborne PM during the sanding of SSC materials, concentrating on differentiating the effects of the SSC material itself from contributions of various sandpaper abrasives (aluminum oxide, ceramic, silicon carbide). Previous work identified pulmonary inflammation and fibrosis risks tied to SSC work and showed *in vivo* inflammation and poor clearance of SSC particles. Building on this, the current study employed an *in vitro* model using human THP-1 macrophages to analyze cellular responses to PM from different sandpapers, compared with responses to abrasive analogue particles and ATH, a primary SSC component.

A key observation was the difference in cellular reactions between the SSC sanding dusts and the abrasive analogue particles. The SSC dusts from all three sandpaper types (SSC Al2O3, SSC Ceramic, SSC SiC) prompted significant apoptosis within THP-1 cells. However, they did not yield significant overt cytotoxicity (LDH release), interfere with cell cycle progression (S phase reduction), or cause mitotic alterations (seen as multinucleation, micronucleation, and NDI changes) at the tested concentration (10 μg/well) and time point (48 h). ATH, representing a major SSC component, also triggered apoptosis, similar to the SSC dusts. This pattern suggests the apoptotic response seen with SSC sanding dusts likely stems from components within the SSC material, like ATH, not primarily from free abrasive particles from the sandpaper. This finding aligns with Kang et al. (2021), who reported that aluminum in PM from sanding SSC mostly originated from the SSC material itself, irrespective of the sandpaper used.

Conversely, the abrasive analogue particles displayed a distinct toxicity profile. Although they generally did not cause substantial LDH release, the Al2O3, ceramic, and SiC abrasive analogue particles significantly lowered the S phase cell percentage, implying cell cycle arrest. These abrasive analogue particles also led to significant increases in multinucleated and micronucleated cells and modified the Nuclear Division Index, indicating considerable interference with mitosis and suggesting genotoxic potential. Ceramic and SiC abrasive analogue particles also elevated necrosis. The potent effects of SiC abrasive analogue particles—inducing high levels of apoptosis and significant rises in binucleated/multinucleated cells—deserve attention. The fact that these effects (S phase reduction, mitotic disruption) were evident with abrasive analogue particles but absent with the actual SSC sanding dusts strongly implies either that the concentration of free, bioactive abrasive particles in the collected dust was too low to cause these responses, or that the properties of abrasive particles possibly embedded in the SSC dust matrix differ from the abrasive analogue particles.

These *in vitro* observations help refine the understanding of SSC-related lung disease. When SSC dusts and ATH trigger apoptosis, they mimic the mechanisms of other harmful particles like silica, which may lead to inflammation as macrophage apoptosis can release pro-inflammatory signals. Still, the absence of significant LDH release or mitotic changes from SSC dusts during this 48-hour assay conflicts with the substantial inflammation, granuloma development, and possible fibrosis seen in *in vivo* and human cases. This difference highlights the limitations of using short-term *in vitro* tests to model chronic *in vivo* reactions. It is important to note that while our collection system used a cyclone with a 5 μm cut-point, the resulting MMAD of the dust was approximately 2.8 μm (Fig. 1), with a substantial fraction of the particle mass residing in a size range capable of penetrating to the deep lung. Therefore, the use of an alveolar macrophage model is highly relevant for assessing the biological effects of this specific dust profile. Fibrosis is a complicated, long-term process that involves persistent inflammation, frustrated phagocytosis, and the sustained activation of multiple cell types—factors that were likely inactive or not apparent in this simplified system or timeframe. Our previous work also showed size-dependent toxicity *in vitro*; while this study used the respirable fraction, its particular size distribution could affect the results compared to the abrasive analogue particles.

Concerning the question raised earlier about whether pulmonary fibrosis might stem from SSC's ATH or sandpaper's Al2O3, our current results point toward SSC components (like ATH) as the main driver of the initial *in vitro* apoptotic response from sanding dust. The separate and more severe effects on cell cycle and mitosis from Al2O3 abrasive analogue particles were not replicated by dust from Al2O3 sandpaper. This doesn't exclude a role for Al2O3 or other abrasives in chronic *in vivo* conditions, perhaps via different mechanisms or synergistic effects not observed here.

Limitations of this work include using a single cell line (THP-1), which might not fully represent primary human AMs or the complex lung microenvironment that includes other critical cell types like epithelial cells. The study also used a single, sub-lethal dose and a 48 h exposure, which may not capture the full dynamics of chronic occupational exposure where cumulative dose and particle persistence are vital. Furthermore, our focus was on cell viability and mitotic disruption; a crucial next step would be to evaluate other pathways, such as the expression of inflammatory cytokines, to better understand the pro-inflammatory potential of these dusts.

Taken together, this study suggests that *in vitro*, respirable dust from sanding SSC primarily induces macrophage apoptosis attributable to SSC components, irrespective of the sandpaper used. Abrasive analogue particles, however, cause more pronounced effects on cell cycle and mitosis, effects not seen with the mixed SSC sanding dust in these experiments. These findings highlight the intrinsic toxicity of the SSC material in the initial cellular response, although the complex pathology seen *in vivo* likely involves chronic mechanisms, possibly involving particle characteristics not fully reproduced here. Future work could examine longer exposures, different dose levels, particle properties within the dust matrix, and perhaps more involved *in vitro* models or *in vivo* comparisons to further clarify the processes driving SSC-associated lung disease.

Disclaimer

The findings and conclusions in this report are those of the authors and do not necessarily represent the official position of the National Institute for Occupational Safety and Health (NIOSH), Centers for Disease Control and Prevention (CDC). Mention of any company or product does not constitute endorsement by NIOSH/CDC.

Funding

National Institute for Occupational Safety and Health project 93909NF.

CRediT authorship contribution statement

Sarah Keeley: Writing – review & editing, Investigation. **Yong Qian:** Writing – review & editing, Funding acquisition, Conceptualization. **Chaolong Qi:** Writing – review & editing, Conceptualization. **Alycia Knepp:** Writing – review & editing, Investigation. **Eun Gyung**

Lee: Writing – review & editing, Methodology, Investigation, Conceptualization. **Seungkoo Kang:** Writing – review & editing, Methodology. **W. Kyle Mandler:** Writing – review & editing, Writing – original draft, Supervision, Project administration, Methodology, Investigation, Funding acquisition, Formal analysis, Data curation, Conceptualization. **Mckinney Walter:** Writing – review & editing, Writing – original draft, Methodology, Investigation.

Declaration of Competing Interest

The authors declare the following financial interests/personal relationships which may be considered as potential competing interests: W. Kyle Mandler reports financial support was provided by National Institute for Occupational Safety and Health project 93909NF. If there are other authors, they declare that they have no known competing financial interests or personal relationships that could have appeared to influence the work reported in this paper.

Data availability

Data will be made available on request.

References

Arredouani, M.S., Yang, Z., Imrich, A., Ning, Y., Qin, G., Kobzik, L., 2006. The macrophage scavenger receptor SR-AI/II and lung defense against pneumococci and particles. Am. J. Respir. Cell Mol. Biol. 35 (4), 474–478.

Becker, S., Fenton, M.J., Soukup, J.M., 2002. Involvement of microbial components and Toll-Like receptors 2 and 4 in cytokine responses to air pollution particles. Am. J. Respir. Cell Mol. Biol. 27 (5), 611–618.

Chew, R., Nigam, S., Sivakumaran, P., 2016. Alveolar proteinosis associated with aluminium dust inhalation. Occup. Med. 66 (6), 492–494.

DuPont, 2018. Corian Solid Surface Product Overview. Corian Design, Wilmington, DE.

Hamilton, R.F., Thakur, S.A., Holian, A., 2008. Silica binding and toxicity in alveolar macrophages. Free Radic. Biol. Med. 44 (7), 1246–1258.

Hiura, T.S., Kaszubowski, M.P., Li, N., Nel, A.E., 1999. Chemicals in diesel exhaust particles generate reactive oxygen radicals and induce apoptosis in macrophages. J. Immunol. 163 (10), 5582–5591.

Hogg, J.C., Van Eeden, S., 2009. Pulmonary and systemic response to atmospheric pollution. Respirology 14 (3), 336–346.

Hubbard, R., Cooper, M., Antoniak, M., Venn, A., Khan, S., Johnston, I., Lewis, S., Britton, J., 2000. Risk of cryptogenic fibrosing alveolitis in metal workers. Lancet 355 (9202), 466–467.

Jederlinic, P.J., Abraham, J.L., Churg, A., Himmelstein, J.S., Epler, G.R., Gaensler, E.A., 1990. Pulmonary fibrosis in aluminum oxide workers: investigation of nine workers, with pathologic examination and microanalysis in three of them. Am. Rev. Respir. Dis. 142 (5), 1179–1184.

Kang, S., Liang, H., Qian, Y., Qi, C., 2021. "The composition of emissions from sanding Corian® with different sandpapers. Aerosol Air Qual. Res. 21, 1–8.

Mandler, W.K., Kang, S., Farcas, M., Qi, C., Friend, S.A., Qian, Y., 2020. *in vitro* toxicity assessment of respirable solid surface composite sawing particles. Toxicol. Ind. Health 36 (4), 250–262.

Mandler, W.K., Qi, C., Orandle, M.S., Sarkisian, K., Mercer, R.R., Stefaniak, A.B., Knepp, A.K., Bowers, L.N., Battelli, L.A., Shaffer, J., Friend, S.A., Qian, Y., Sisler, J. D., 2019. Mouse pulmonary response to dust from sawing Corian(R), a Solid-Surface composite material. J. Toxicol. Environ. Health Part A 82 (11), 645–663.

Mandler, W.K., McKinney, W.G., Jackson, M., Knepp, A.K., Keeley, S.L., Friend, S.A., Battelli, L.A., Qian, Y., 2025. Mouse pulmonary response following solid surface composite dust inhalation. Inhal. Toxicol. 37 (1), 18–30. https://doi.org/10.1080/08958378.2024.2447699. Epub 2025 Jan 22. PMID: 39841048; PMCID: PMC12077238.

McKeever, R., Okaneku, J., LaSala, G.S., 2014. More on pulmonary fibrosis associated with aluminum trihydrate (Corian) dust. N. Engl. J. Med. 371 (10), 973.

McKinney, W., Chen, B., Schwegler-Berry, D., Frazer, D.G., 2013. Computer-Automated silica aerosol generator and animal inhalation exposure system. Inhal. Toxicol. 25 (7), 363–372.

Mukae, H., Hogg, J.C., English, D., Vincent, R., Van Eeden, S.F., 2000. Phagocytosis of particulate air pollutants by human alveolar macrophages stimulates the bone marrow. Am. J. Physiol. Lung Cell. Mol. Physiol. 279 (5), L924–L931.

Raghu, G., Collins, B.F., Xia, D., Schmidt, R., Abraham, J.L., 2014. Pulmonary fibrosis associated with aluminum trihydrate (Corian) dust. N. Engl. J. Med. 370 (22), 2154–2156.

Taskar, V.S., Coultas, D.B., 2006. Is idiopathic pulmonary fibrosis an environmental disease? Proc. Am. Thorac. Soc. 3 (4), 293–298.